



Published in final edited form as:

*Biomaterials*. 2009 February ; 30(4): 478–483. doi:10.1016/j.biomaterials.2008.10.019.

## Controlled remineralization of enamel in the presence of amelogenin and fluoride

Yuwei Fan<sup>+</sup>, Zhi Sun, and Janet Moradian-Oldak<sup>\*</sup>

Center for Craniofacial Molecular Biology, University of Southern California, 2250 Alcazar Street, CSA103, HSC, Los Angeles, CA 90033

### Abstract

Reconstructing enamel-like structures on teeth has been an important topic of study in the material sciences and dentistry. The important role of amelogenin in modulating the mineralization of organized calcium phosphate crystals has been previously reported. We used amelogenin and utilized a modified biomimetic deposition method to remineralize the surface of etched enamel to form mineral layers containing organized needle-like fluoridated hydroxyapatite crystals. The effect of a recombinant amelogenin (rP172) on the microstructure of the mineral in the coating was analyzed by SEM, XRD and FT-IR. At rP172 concentrations below 33  $\mu\text{g/mL}$ , no significant effect was observed. In the presence of 1 mg/L F and at a concentration of 33  $\mu\text{g/mL}$  rP172, formation of fused crystals growing from the enamel surface was initiated. Amelogenin promoted the oriented bundle formation of needle-like fluoridated hydroxyapatite in a dose dependent manner. Biomimetic synthesis of the amelogenin fluoridated hydroxyapatite nano-composite is one of the primary steps towards the development and design of novel biomaterial for future application in reparative and restorative dentistry.

### Keywords

amelogenin; fluoride; enamel remineralization; fluoridated hydroxyapatite

### Introduction

The highly organized hierarchical microstructure provides dental enamel its high strength and anti-abrasive properties [1]. Mature enamel is acellular, has more than 95% mineral content and does not remodel. The crystals found in enamel are carbonated hydroxyapatite nanocrystals, 50–70 nm in width, 20–25 nm in thickness, with length to width aspect ratio over 1000. Enamel has a high packing density of inorganic material, evident when comparing enamel density (2.85–3.00  $\text{g/cm}^3$ ) [2] to pure monolith HAP (3.08  $\text{g/cm}^3$ ). Recent approaches for *in vitro* synthesis of enamel-like hydroxyapatite (HAP) nanorods include: hydrothermal method with control release of calcium from Ca-EDTA [3], hydrothermal transformation of octacalcium phosphate (OCP) rod to HAP nanorods in the presence of gelatin [4], surfactant supported HAP self-assembly [5,6], hydrogen peroxide containing calcium phosphate paste

\*Corresponding author: Janet Moradian-Oldak, Address: 2250 Alcazar Street, CSA103, HSC, Los Angeles, CA 90033, USA, Tel: +1-(323)-442-1759, Fax: +1-(323)-442-2981, Email: joldak@usc.edu.

<sup>+</sup>Yuwei Fan, Current address: School of Dentistry, Louisiana State University Health Science Center. 1100 Florida Ave, Box-137, New Orleans, LA 70119

**Publisher's Disclaimer:** This is a PDF file of an unedited manuscript that has been accepted for publication. As a service to our customers we are providing this early version of the manuscript. The manuscript will undergo copyediting, typesetting, and review of the resulting proof before it is published in its final citable form. Please note that during the production process errors may be discovered which could affect the content, and all legal disclaimers that apply to the journal pertain.

[7] and electrolytical deposition taking place at 85°C [8]. The majority of these synthesis methods were developed under the condition of high temperature, high pressure, extreme acidic pH or in the presence of a concentrated solution of surfactants. The investigation of *in vitro* biomimetic synthesis of enamel-like calcium phosphate structures under physiological conditions is therefore essential in dentistry as an alternative dental restorative material. However, the synthesis of rod-like apatite crystals under physiological temperature is a challenging task. *In vitro* formation of enamel-like apatite crystals under relatively mild conditions was reported for the first time by Moriwaki et al., [9] in a mineralization device using a cation-selective membrane system. In such a device the direction of calcium ion transport was controlled and the crystals formed in the membrane isolated chamber contained bundles of needle-like OCP and HAP. Using a similar system, Iijima et al. applied a dual-membrane device as a model of enamel formation to investigate the function of amelogenin proteins on calcium phosphate mineralization [10,11]. The co-existence of amelogenin and fluoride (F) was found to be crucial for the organized rod-like apatite crystal formation on the membrane [11,12].

In enamel mineralization, supermolecular assembly of the extracellular macromolecules is a crucial step [13]. The amelogenin-rich extracellular organic matrix of enamel is continuously secreted, assembled, processed, and mineralized during enamel development. Amelogenin self-assembly is believed to be a key factor in controlling the oriented and elongated growth of the carbonate-containing fluoridated hydroxyapatite crystals within enamel prisms. Numerous *in vitro* experimental approaches have been implemented to demonstrate amelogenin's ability to control particular aspects of calcium phosphate mineralization (nucleation, crystal morphology and orientation) [14–19].

We have recently applied an electrolytic deposition (ELD) system to promote the amelogenin self-assembly and simultaneous calcium phosphate crystallization [18] as a basis for the design and development of enamel-like material. SEM observation of the surface of the nano-composite, prepared by ELD in the presence of a recombinant pig full-length amelogenin (rP172) on Si wafer surface, revealed organized nano-rod structures, while only nano-sized spherical aggregates were seen in the presence of a truncated amelogenin lacking the hydrophilic C-terminal domain (rP148). We have therefore concluded that the full-length amelogenin was essential for the growth of organized structures on the surface of the cathode and that its self-assembly was the driving force for crystal organization [18].

Based on our previous findings, we further implemented a modified biomimetic mineralization approach to rebuild the enamel structure on an acid etched enamel surface as an early caries model. Using a biomimetic mineralization method, we found that fluoride had a significant effect on the calcium phosphate crystal morphology in the remineralization of enamel crystals. The needle-shaped nanocrystals grew on acid etched enamel (unpublished data). In this report, we investigate the effect of amelogenin on the crystal growth on enamel, and demonstrate the successful preparation of biocomposite coating when oriented nano-sized apatite mineralization was mediated by the presence of fluoride and recombinant amelogenin. The present biomimetic synthesis is one of the primary steps towards the development and design of novel biomaterial for future application in reparative and restorative dentistry.

## Materials and Methods

### Amelogenin preparation

Purified recombinant porcine amelogenin full-length rP172 was prepared as described previously [20]. The rP172 protein has 172 amino acids and is an analogue to the full-length native porcine P173, but lacking the N-terminal methionine and a phosphate group on Ser16. The proteins were expressed in *Escherichia Coli* strain BL21-codon plus (DE3-RP, Strategene,

La Jolla, CA), and purified by ammonium sulfate precipitation, and reverse-phase high performance liquid chromatography (HPLC, C4-214TP510 column, Vydac, Hesperia, CA).

### Tooth slices preparation

Human third molars (extracted following the standard procedures for extraction at the School of Dentistry in University of Southern California and handled with permit by Institutional Review Board) were selected without fillings. The teeth were treated with 3% sodium hypochlorite to remove bacteria and rinsed with phosphate buffered saline (PBS). Slices, 0.2–0.5 mm in thickness, were cut longitudinally or transversely by low speed diamond saw cooled by water. The tooth slices were stored at 4°C in PBS prior to use.

### Biomimetic Coating preparation

The coating was prepared by immersing the tooth slice in the biomimetic calcification solution with 2.58 mM calcium ( $\text{CaCl}_2 \cdot 2\text{H}_2\text{O}$ , >74.4%  $\text{CaCl}_2$ , Curtin Matheson Scientific, Houston, TX) and 1.55 mM phosphates ( $\text{KH}_2\text{PO}_4$ , >99%, EM Science, Gibbstown, NJ) at 37°C, buffered by 50 mM pH=7.6 trihydroxymethylaminomethane (Tris) – hydrochloric acid and 180 mM NaCl. The calcification solution pH was adjusted by 1 M HCl to 7.60 using a Metrohm 718 pH-STAT. The tooth slice was etched by 3%  $\text{HNO}_3$  solution for 50 seconds, rinsed with sufficient deionized water and immediately immersed in 12 mL freshly prepared biomimetic calcification solution. Fluoride from NaF (>99%, Sigma-Aldrich, St. Louis, MO) was added to obtain the final desirable concentrations of fluoride, 1mg/L, just before the immersing tooth slice. The mineralization solution was air-tightly sealed in a 20 mL scintillation vial and incubated at 37°C statically for 2–30 hours. After desired time, the tooth slide was removed from solution, rinsed with running di-ionized water for 50 seconds and air-dried.

### Structural and compositional analysis

The samples with biomimetic coating were sputtered with 5 nm thick carbon for conductivity, and secondary electron images were acquired by a field emission scanning electron microscope (FE-SEM, Leo 1550 VP) at 5kV. The phase composition and orientation of the coating was determined by X-Ray Diffraction (XRD) on a Rigaku Rotaflex RU-200 diffractometer with Cu target at 0.154 nm; the acceleration voltage was 70 kV and current 50 mA. The diffraction intensity was collected from 10~60 degrees at 0.05 degree intervals and processed by the attached computer. The grain size of the crystals was calculated by the Scherrer equation. The half height peak width was calculated after peak separation according to Gaussian fit. FT-IR spectra were acquired from a Jasco FT-IR 2000 system with a Gladi-ATR (Attenuated Total Reflection) diamond crystal accessory (Pike Technology, Madison WI). The sample with coating was pressed on the diamond crystal under about 30,000 psi and scanned at  $4 \text{ cm}^{-1}$  resolution, from  $4000 \text{ cm}^{-1}$  to  $500 \text{ cm}^{-1}$ , 30 times.

### Results and Discussion

Fig 1A shows the SEM image of the enamel surface following acid etching. Enamel crystals at the surface were discontinuous and broken resembling early enamel caries. A calcium phosphate coating was formed on the surface of the tooth following 16 hours of soaking in the biomimetic mineralization solution. As shown in Fig 1B about 50  $\mu\text{m}$  in thickness crack-free calcium phosphate coating was found on the enamel surface. Although the surface of enamel was about 30% or less in the total tooth slice, almost no coating could be found on dentine. The crystals formed on enamel had flake-like structure and the coating was porous (Fig. 1C). Fig 1D shows some isolated flake-like cluster on dentin that can be found around the inter-tubular dentin matrix. Due to the inhibitory nature of collagen-rich surface of dentine, compared to mineral-rich enamel surface, the calcium phosphate formation on dentin is not favorable in this system.

ATR FT-IR (Fig. 2) and XRD (Fig. 3) spectra indicated that the mineral phase of the calcium phosphate coating without fluoride was mainly OCP, along with some HAP. FT-IR in Fig. 2 demonstrated the presence of protein and phosphate mineral on the remineralization coating prepared with amelogenin. In the presence of amelogenin, the minerals were mainly OCP without fluoride and turned to be HAP after adding 1 mg/L fluoride. The  $\text{PO}_4$  band indicates the biomimetic coating of calcium phosphate with amelogenin ( $600$  and  $558\text{ cm}^{-1}$ ) is different than HAP standard at  $601$  and  $563\text{ cm}^{-1}$  [18,21]. The composite coating with fluoride shows  $601$ ,  $554\text{ cm}^{-1}$  band, close to enamel surface absorbance at  $602$  and  $548$ ,  $533\text{ cm}^{-1}$ . Such blue shift may be the overlap of fluoridated HAP and OCP when the HAP layer is grown on the laminar OCP precursor in the presence of F as the structure disclosed by Iijima et al [22].

To estimate the preferable orientation degree of the crystals, the intensity of diffraction peak (002) at  $2\theta=25.8$ , (211) at  $2\theta=31.8$ , (112) at  $2\theta=32.2$ , and (300) at  $2\theta=32.8$  were calculated by peak separation process according to Gaussian fit. The intensities of HAP diffractions corresponding to (002), (300) and (211) peaks were measured and the ratio of diffraction intensity of z axis (002) to another direction was used to describe the orientation degree. XRD spectra were shown in Fig. 3 by comparing the biomimetic coating prepared in the presence of different concentrations of rP172. The typical crystal size for CaP nanorod was estimated around 25 nm in diameter (based on the broadening of 300 or 211 direction) and 100 nm in length (based on the broadening of 002 direction), which matched the dimensions observed from SEM. From XRD results after Gaussian Fit, the (002) to (211) intensity ratio for enamel control is 0.37, for CaP/F/rP172 coating 1.38 and for CaP/F coating 1.06. As JCPDF #09-0432 for hydroxyapatite, intensity ratio of (002) to (211) is 0.4. This indicated the preferential orientation of the calcium phosphate coating was significantly improved with the presence of rP172 and F.

The effect of rP172 on the mineral morphology was analyzed under different concentrations of rP172. In general, calcium phosphate crystal growth in the coating was suppressed by the addition of rP172, as shown in Fig. 4. The plate-like calcium phosphate crystals become shorter after adding amelogenin. At  $20\text{ }\mu\text{g/mL}$  rP172, the straight plate-like crystals became curved crystals as shown in Fig 4C. At  $70\text{ }\mu\text{g/mL}$  (Fig. 4D) and  $100\text{ }\mu\text{g/mL}$  (Fig. 4E) amelogenin, the crystals were more curved and some of the curved plates tended to align together with their c-axis parallel to each other. Similar bundles of organized crystals grown in solution in the presence of rP172 (Fan et al. unpublished data), or rM179 [16] were also observed. XRD spectrum of the mineral in the coating indicated the presence of HAP crystals (Fig. 4F). The addition of amelogenin did not appear to affect the mineral phase, however, the increased diffusion peak at  $2\theta=16\text{--}22$  degree may indicate the presence of amorphous calcium phosphate. This broadening could also be the result of the appearance of smaller apatite crystals.

To mimic the enamel nano-rod bundles, the effect of rP172 in the presence of 1mg/L fluoride was investigated. In the presence of 1 mg/L fluoride ions, the crystals were needle-like fluoridated hydroxyapatite [19]. As shown in Fig. 5, the packing density of needle-like crystal coating increased with the concentration of rP172 after 16 hours deposition. At control or  $10\text{ }\mu\text{g/mL}$  rP172, the crystal are isolated and separated. At the concentration of  $33\text{ }\mu\text{g/mL}$  rP172, the isolated needle-like crystals formed crossed linkages and some bundles (Fig 5C). At  $70\text{ }\mu\text{g/mL}$  rP172, the needle-like crystals bundled together forming a coating with a high mineral pack density (Fig 5D).

The progression of crystal growth observed with time lapse at 2, 4, 6, 8, 12, 16 hours in the presence of  $33\text{ }\mu\text{g/mL}$  rP172 is shown in Fig. 6. At 2 hours (Fig. 6A), the epitaxial growth has occurred and no significant overgrowth was found. The surface of enamel crystal is smooth without indent and discontinuity. At 4 hours (Fig. 6B), the overgrowth of the branched crystals can be found on the pre-existing enamel crystals. After 6–8 hours (Figs 6C, D), the formation

of rod-like crystals was significant. After 12–16 hours (Fig 6E and F), the continuous coating of the HAP needle array was formed. The needle-like apatite crystals were aligned with their c-axis perpendicular to the substrate, measuring 20 nm in diameter and over 200 nm in length. The bundled crystal formed at about 6 hours mineralization.

## CONCLUSIONS

We found that the minimum concentration of recombinant amelogenin rP172 required to mediate the organized crystal bundle formation in a calcification system, under physiological pH and temperature conditions is around 33  $\mu\text{g}/\text{mL}$ . Amelogenin promoted the oriented bundle formation of needle-like fluoridated hydroxyapatite in a dose dependent manner. We demonstrated that tuning the crystal packing density and remineralization can be controlled by application of amelogenin and by incorporation of fluoride. The synthetic nano-rod and organized bundled crystals formed on etched enamel in the presence of amelogenin have potential application in restorative dentistry and prevention of carries progression. The biomimetic coating of fluoridated calcium phosphate has excellent biocompatibility with enamel and dentin. Therefore, we propose that for repairing the mineral loss caused by early caries lesions the *in situ* remineralization of enamel in the presence of amelogenin is a promising approach.

## References

1. Boyde, A. Microstructure of enamel. In: Chadwick, DJ.; Cardew, G., editors. Dental Enamel: Ciba Foundation Symposium 205. New York: John Wiley & Sons; 1997. p. 18-31.
2. Manly RS, Hodge HC, Ange LE. Density and refractive index studies of dental hard tissues. II. Density distribution curves. J Dent Res 1939;18(3):203–211.
3. Chen HF, Tang ZY, Liu J, Sun K, Chang S-R, Peters MC, et al. Acellular synthesis of a human enamel-like microstructure. Adv Mater 2006;18(14):1846–51.
4. Zhan JH, Tseng YH, Chan JC, Mou CY. Biomimetic formation of hydroxyapatite nanorods by a single-crystal-to-single-crystal transformation. Adv Funct Mater 2005;15:2005–2010.
5. Chen HF, Clarkson BH, Sun K, Mansfield JF. Self-assembly of synthetic hydroxyapatite nanorods into an enamel prism-like structure. J Colloid Interface Sci 2005;288(1):97–103. [PubMed: 15927567]
6. Fowler CE, Li M, Mann S, Margolis HC. Influence of surfactant assembly on the formation of calcium phosphate materials - A model for dental enamel formation. J Mater Chem 2005;15(32):3317–25.
7. Onuma K, Yamagishi K, Oyane A. Nucleation and growth of hydroxyapatite nanocrystals for nondestructive repair of early caries lesions. J Crystal Growth 2005;282(1–2):199–207.
8. Ye W, Wang XX. Ribbon-like and rod-like hydroxyapatite crystals deposited on titanium surface with electrochemical method. Mater Letter 2007;61(19–20):4062–4065.
9. Moriwaki, Y.; Doi, Y.; Kani, T.; Aoba, T.; Takahashi, J.; Okazaki, M. Synthesis of enamel-like apatite at physiological temperature and pH using ion-selective membranes. In: Suga, S., editor. Mechanisms of tooth enamel formation. Tokyo Japan: Quintessence Publishing Co; 1983. p. 239-256.
10. Iijima M, Moriwaki Y, Wen HB, Fincham AG, Moradian-Oldak J. Elongated growth of octacalcium phosphate crystals in recombinant amelogenin gels under controlled ionic flow. J Dent Res 2002;81(1):69–73. [PubMed: 11820371]
11. Iijima M, Moradian-Oldak J. Control of apatite crystal growth in a fluoride containing amelogenin-rich matrix. Biomaterials 2005;26(13):1595–1603. [PubMed: 15522761]
12. Iijima M, Du C, Abbott C, Doi Y, Moradian-Oldak J. Control of apatite crystal growth by the cooperative effect of a recombinant porcine amelogenin and fluoride. Eur J Oral Sci 2006;114(Suppl): 304–307. [PubMed: 16674703]
13. Fincham AG, Moradian-Oldak J, Simmer JP. The structural biology of the developing dental enamel matrix. J Struct Biol 1999;126(3):270–299. [PubMed: 10441532]
14. Wen HB, Moradian-Oldak J, Fincham AG. Modulation of apatite crystal growth on Bioglass (R) by recombinant amelogenin. Biomaterials 1999;20(18):1717–1725. [PubMed: 10503973]

15. Iijima M, Moradian-Oldak J. Control of octacalcium phosphate and apatite crystal growth by amelogenin matrices. *J Mater Chem* 2004;14(14):2189–2199.
16. Beniash E, Simmer JP, Margolis HC. The effect of recombinant mouse amelogenins on the formation and organization of hydroxyapatite crystals in vitro. *J Struct Biol* 2005;149(2):182–190. [PubMed: 15681234]
17. Wang LJ, Guan XY, Yin HY, Moradian-Oldak J, Nancollas GH. Mimicking the self-organized microstructure of tooth enamel. *J Phys Chem C* 2008;112(15):5892–5899.
18. Fan YW, Sun Z, Wang R, Abbott C, Moradian-Oldak J. Enamel inspired nanocomposite fabrication through amelogenin supramolecular assembly. *Biomaterials* 2007;28(19):3034–3042. [PubMed: 17382381]
19. Habelitz S, Kullar A, Marshall SJ, DenBesten PK, Balooch M, Marshall GW, Li W. Amelogenin-guided crystal growth on fluoroapatite glass-ceramics. *J Dent Res* 2004;83(9):698–702. [PubMed: 15329375]
20. Ryu OH, Fincham AG, Hu CC, Zhang C, Qian Q, Bartlett JD, Simmer JP. Characterization of recombinant pig enamelysin activity and cleavage of recombinant pig and mouse amelogenins. *J Dent Res* 1999;78(3):743–50. [PubMed: 10096449]
21. Koutsopoulos S. Synthesis and characterization of hydroxyapatite crystals: A review study on the analytical methods. *J Biomed Mater Res* 2002;62(4):600–612. [PubMed: 12221709]
22. Iijima M, Tohda H, Suzuki H, Yanagisawa T, Moriwaki Y. Effect of F- on apatite-octacalcium phosphate intergrowth and crystal morphology in a model system of tooth enamel formation. *Calcif Tissue Int* 1992;50(4):357–361. [PubMed: 1571848]

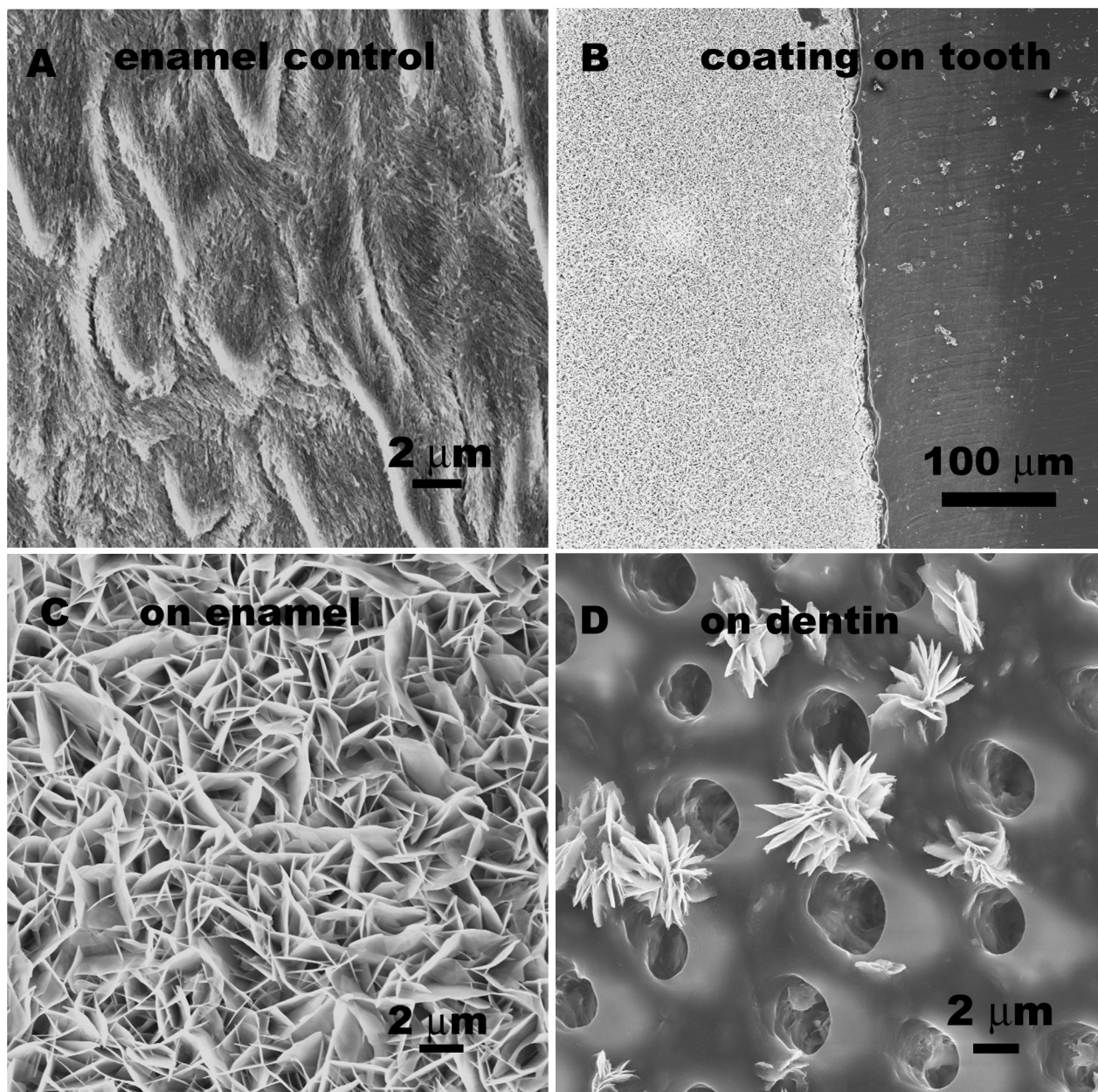


**Fig. 1.** SEM images of A) enamel surface after acidic etching, B) biomimetic mineralization coating, the left white region, formed on enamel surface in calcium phosphate containing solution after 16 hours. There is no continuous coating on dentine surface (the dark area on the right). As seen under higher magnification, C) the calcium phosphate coating grew on left enamel surface part and D) isolated crystals were found on right dentin part. The round holes are dentine tubules.

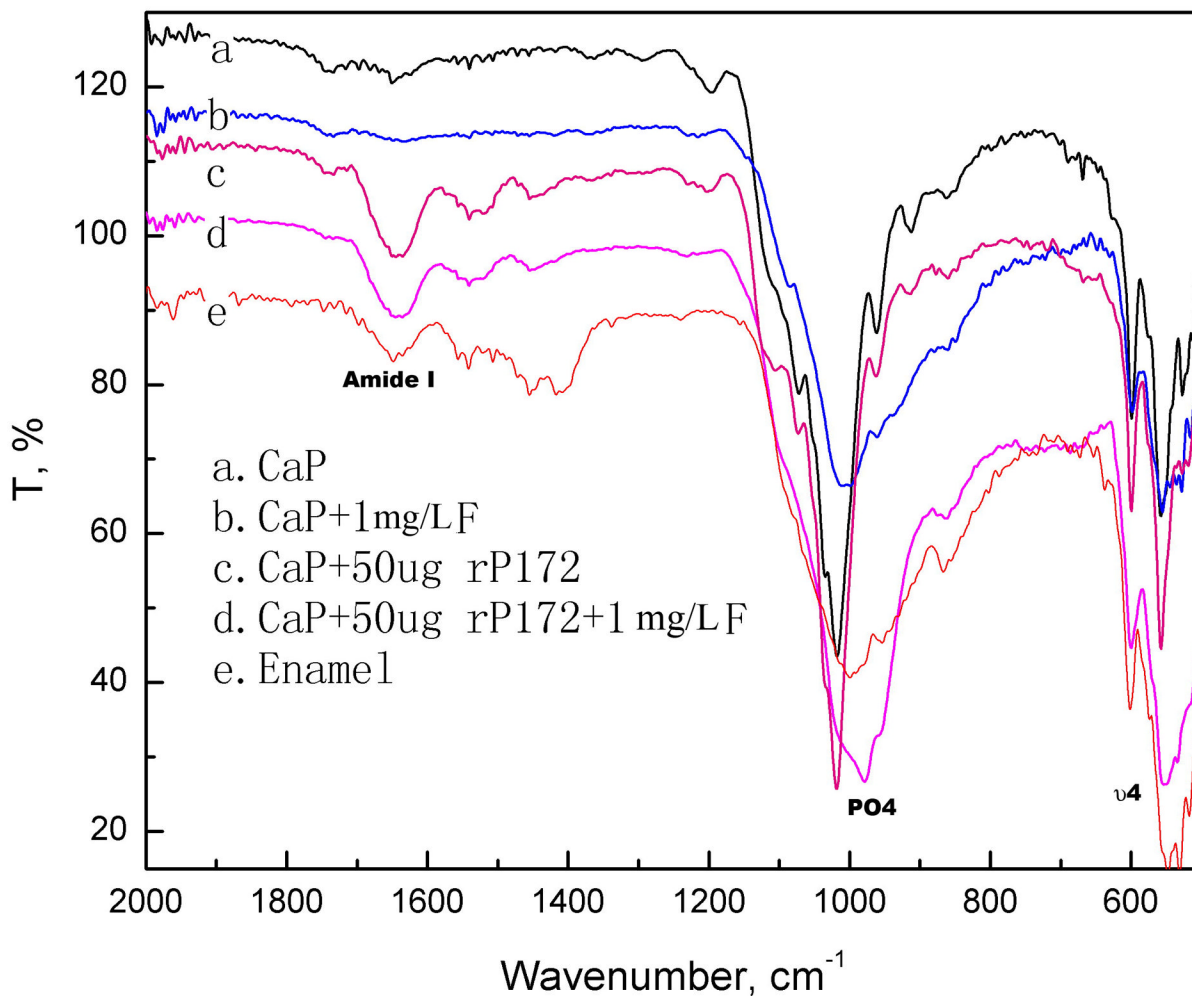


**Fig. 2.**

ATR FT-IR spectrum of the biomimetic coating on enamel prepared after 16 hours compared with enamel control. The presence of protein amide I band at  $1680\text{ cm}^{-1}$  in the composite coating with rP172 was significant. The mineral phase of the calcium phosphate coating was mainly OCP. Spectrum of coating with fluoride and rP172 was close to native enamel, which was fluoridated HAP.



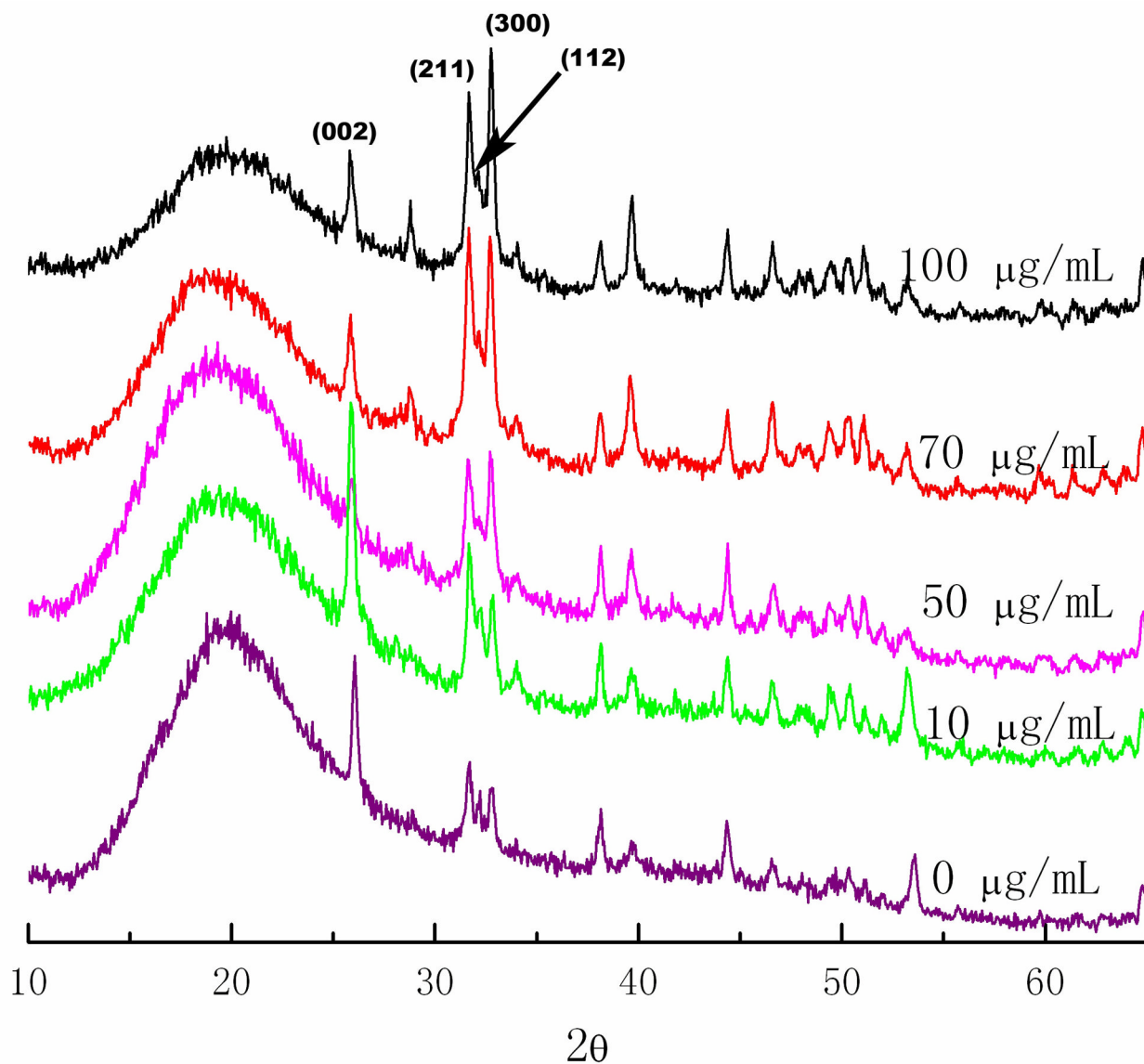


**Fig. 3.** The XRD spectrum of the biomimetic coating on enamel with 1mg/L F and concentrations of rP172 amelogenin of 0, 10, 50, 70, 100  $\mu\text{g/mL}$ . The presence of hydroxyapatite diffraction band (002) at  $2\theta=12.9$ , (211) at  $2\theta=15.9$ , (112) at  $2\theta=16.1$ , and (300) at  $2\theta=16.4$  were clearly detected. The addition of rP172 didn't alter the HAP phase significantly.

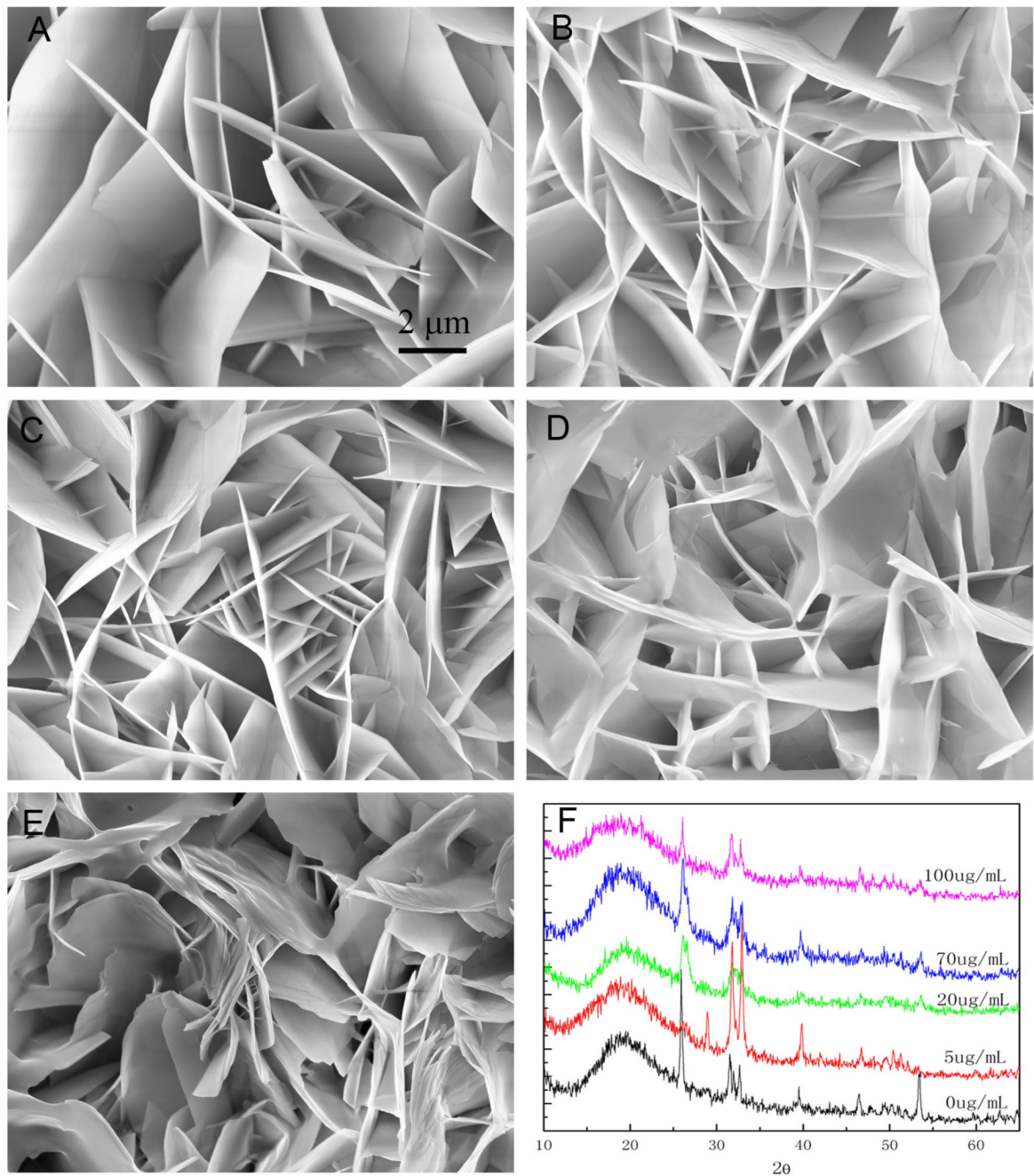


**Fig. 4.** SEM images of calcium phosphate coating prepared on enamel surface after 16 hours with different concentrations of rP172 amelogenin: A) 0, B) 5  $\mu\text{g}/\text{mL}$ , C) 20  $\mu\text{g}/\text{mL}$ , D) 70  $\mu\text{g}/\text{mL}$ , E) 100  $\mu\text{g}/\text{mL}$  and F) XRD spectrum of the coatings formed at different concentration of rP172.

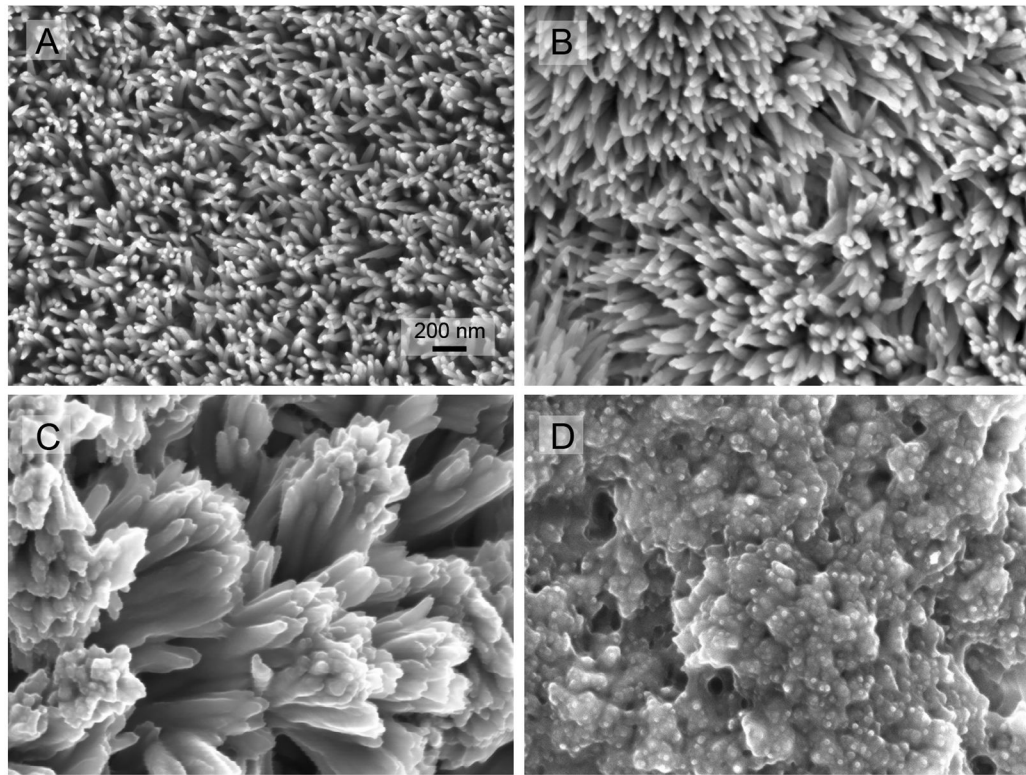


**Fig. 5.** SEM images of fluoridated apatite-amelogenin coatings prepared on enamel surface (longitudinal sections) with 0 (A), 20 (B), 33 (C) and 70 $\mu$ g/mL (D) of rP172 amelogenin in the mineralization solution and 1 mg/L F. All the images were taken under the same magnification.

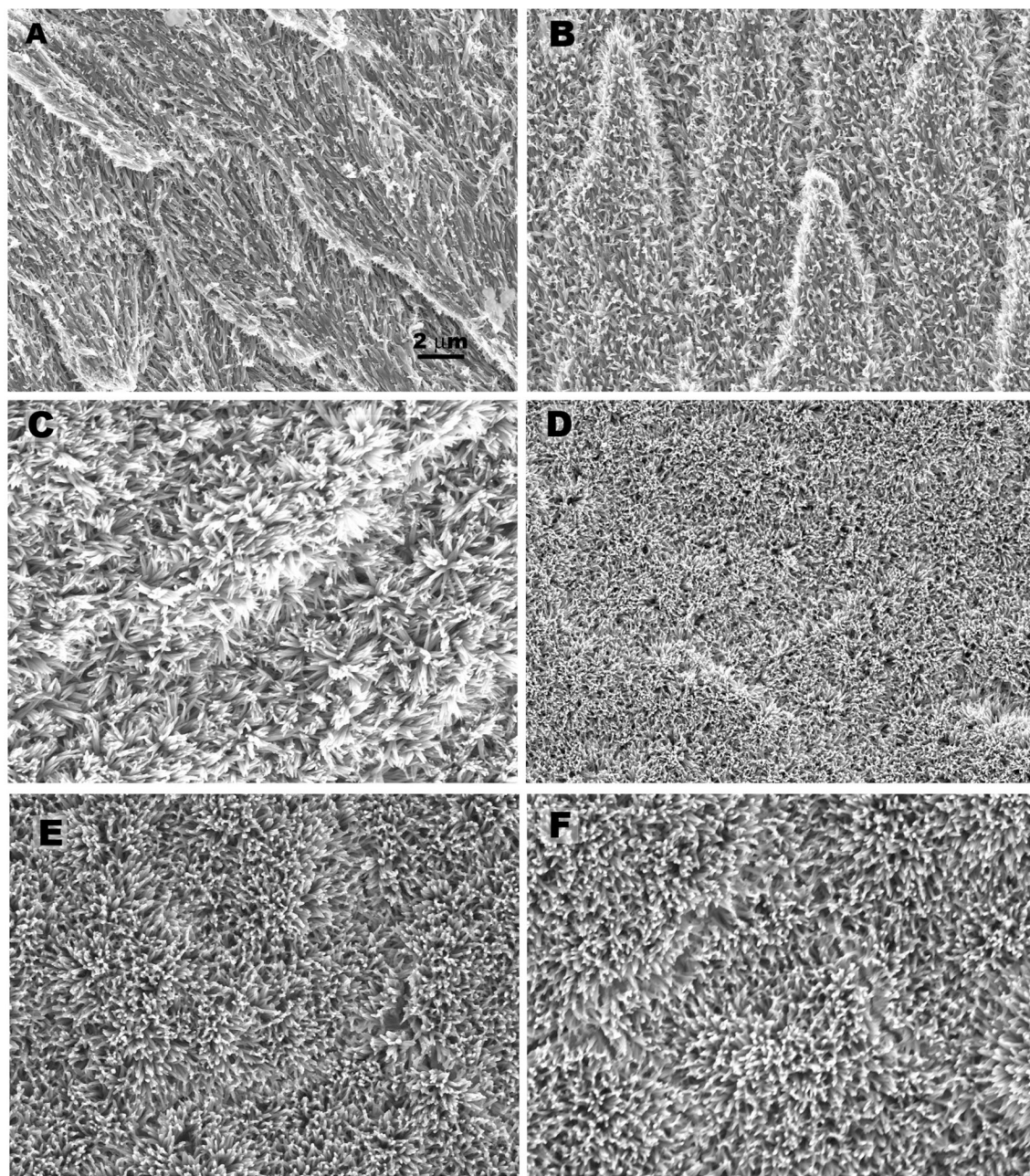


**Fig 6.** SEM images under magnification of 10K showing the progress of crystal growth in the presence of 1 mg/L F and 33  $\mu\text{g/mL}$  rP172 at the reaction time of 2 (A), 4 (B), 6 (C), 8(D), 12 (E) 16(F) hours. Control at zero hour is shown in Fig. 1A.